

Reward Informed Dreamer for Task Generalization in Reinforcement Learning

Chengyang Ying¹ Zhongkai Hao¹ Xinning Zhou¹ Hang Su¹ Songming Liu¹ Jialian Li¹ Dong Yan¹
Jun Zhu¹

Abstract

A long-standing goal of reinforcement learning is that algorithms can learn on training tasks and generalize well on unseen tasks like humans, where different tasks share similar dynamic with different reward functions. A general challenge is that it is nontrivial to quantitatively measure the similarities between these different tasks, which is vital for analyzing the task distribution and further designing algorithms with stronger generalization. To address this, we present a novel metric named Task Distribution Relevance (TDR) via optimal Q functions to capture the relevance of the task distribution quantitatively. In the case of tasks with a high TDR, i.e., the tasks differ significantly, we demonstrate that the Markovian policies cannot distinguish them, yielding poor performance accordingly. Based on this observation, we propose a framework of Reward Informed Dreamer (RID) with reward-informed world models, which captures invariant latent features over tasks and encodes reward signals into policies for distinguishing different tasks. In RID, we calculate the corresponding variational lower bound of the log-likelihood on the data, which includes a novel term to distinguish different tasks via states, based on reward-informed world models. Finally, extensive experiments in DeepMind control suite demonstrate that RID can significantly improve the performance of handling different tasks at the same time, especially for those with high TDR, and further generalize to unseen tasks effectively.

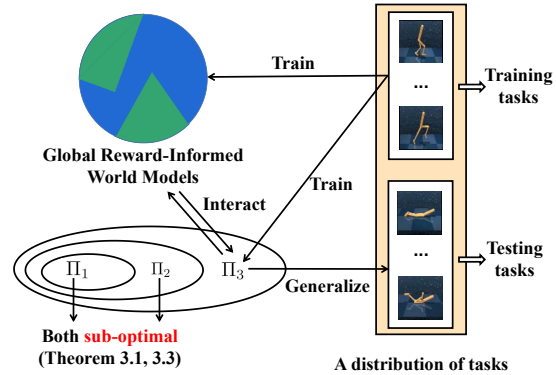


Figure 1. An overview. Given a distribution of tasks, we train the agent in training tasks and hope it generalize to testing tasks. As for hypothesis sets, we show that Π_1 of Markovian policies and Π_2 that encodes historical state-actions are both sub-optimal. For improving the generalization, we propose RID, which encodes reward signals into policies (Π_3) and utilizes novel reward-informed world models for capturing invariant latent features.

decision problems, such as Atari games (Mnih et al., 2015), board games (Silver et al., 2016) as well as robot manipulation (Kendall et al., 2019). However, current learned agents are always overly specialized to the training task and struggle to generalize to unseen tasks (Zhang et al., 2018; Zhao et al., 2019; Kirk et al., 2021), which limits the application of DRL algorithms to more practical scenarios, since the agent in a general environment can not contact all the tasks at the training stage and needs to generalize to unseen tasks in practice. For example, when designing the self-driving agent, we always hope it handle different tasks, like lane-keeping, overtaking other cars, and so on, in a general environment. And generalization here is significant since it is impossible to fit all the tasks in the training stage.

To improve the agent’s generalization, some prior works have empirically designed some training methodologies, like loss regularization (Igl et al., 2019; Wang et al., 2020), network architecture design (Lee et al., 2019; Raileanu & Fergus, 2021), and data augmentation (Raileanu et al., 2021; Hansen & Wang, 2021). However, the mechanism behind policy generalization to unseen environments remains under-explored. Currently, some work (Ghosh et al., 2021) has shown that generalization to unseen environments, which

1. Introduction

Deep reinforcement learning (DRL) algorithms have made great progress in a large number of complicated sequential

*Equal contribution ¹Dept. of Comp. Sci. & Techn., Institute for AI, BNRist Center, Tsinghua University. Correspondence to: Hang Su <suhanngss@tsinghua.edu.cn>, Jun Zhu <dc-szj@tsinghua.edu.cn>.

are different from training environments, will introduce partial observability, which is caused by agents’ epistemic uncertainty about test environments (Ghosh et al., 2021). Consequently, the hypothesis set of Markovian policies Π_1 is no longer optimal when we consider the generalization since the problem is no longer fully observable. Ghosh et al. (2021) further proposes to use stochastic policies to improve the generalization. Moreover, some work (Lee et al., 2020) also experimentally shows that the hypothesis set Π_2 that encodes historical states and actions can perform better generalization than Markovian policies since they can handle partial observability to some degree.

However, the generalization of policies in a distribution of environments is still studied insufficiently since there are few effective metrics of the environment distribution to measure the performance of agents, which is significant for analyzing and designing algorithms with stronger generalization ability. To address this challenge, in this paper, we consider the setting of task generalization, i.e., different environments own the same transition dynamic and different reward functions. This setting is practical and important since we always hope different agents handle their corresponding tasks in a general environment. In this setting, we first define a novel metric named Task Distribution Relevance (TDR) to capture the relevance of the optimal Q functions over different tasks of the distribution. Moreover, we show that the hypothesis set of Markovian policies Π_1 and the hypothesis set Π_2 that encodes historical states and actions are both *sub-optimal* since they can not distinguish different tasks, and the gap between their performance and the optimal return is related to TDR, i.e., when the TDR of the task distribution is larger, their performance is relatively worse, which is also shown experimentally in Sec. 5.

For task distribution with high TDR, Markovian policies perform and generalize poorly. Thus we propose a novel method named Reward Informed Dreamer (RID) for handling task generalization in DRL. In RID, we first extend world models (Ha & Schmidhuber, 2018; Hafner et al., 2019b;a), which effectively learn the environment dynamics and capture invariant latent features (Sekar et al., 2020; Xu et al., 2022), and propose novel reward-informed world models. To improve the agents’ generalization to unseen tasks, our reward-informed world models aim at handling a distribution of tasks, which is analyzed by a probabilistic graphical model (See Fig. 2), and encoding reward signals into the inference model for distinguishing different tasks. Moreover, we calculate the variational lower bound of the log-likelihood on the data in our model, which includes a novel term for distinguishing different tasks via states. Extensive experiments in DeepMind control suite (Tassa et al., 2018) show that our RID can distinguish different tasks to handle them at the same time via utilizing reward signals and further generalize to unseen tasks effectively,

while previous methods can not distinguish different tasks and perform poorly, especially in tasks with high TDR.

In summary, our contributions are:

- We first propose a novel metric TDR to measure the relevance of a distribution of tasks. After theoretically showing that the Markovian policies are sub-optimal when handling a distribution of tasks, we derive that the gap is related to the corresponding TDR.
- Since Markovian policies show poor performance and generalization in task distribution with high TDR, we propose novel reward-informed world models, which aim at capturing the invariant latent features between different tasks and distinguishing different tasks by encoding reward signals into policies.
- By calculating the corresponding variational lower bound, we propose a novel algorithm named RID for better generalizing to unseen tasks. Extensive experiments show that RID can powerfully handle different tasks meanwhile via receiving different reward signals and demonstrate a strong generalization ability to unseen tasks compared with the alternative baselines.

2. Related Work

Now, we introduce the two most relevant types of works: generalization in RL and world models, since we consider the task generalization in RL and propose RID by extending Dreamer-oriented world models (Hafner et al., 2019a).

2.1. Generalization in Reinforcement Learning

Current Reinforcement Learning methods always fail in generalizing to unseen environments (Zhang et al., 2018; Zhao et al., 2019; Song et al., 2019), which has attracted considerable attention recently in the community. For improving the generalization of current agents, some works have empirically designed some training methodologies, like loss regularization (Cobbe et al., 2019; Igl et al., 2019; Wang et al., 2020), network architecture design (Lee et al., 2019; Raileanu & Fergus, 2021), and data augmentation (Cobbe et al., 2019; Raileanu et al., 2021; Hansen & Wang, 2021). Currently, some researchers propose to utilize the strong expression ability of transformer (Vaswani et al., 2017) to train a generalist agent (Reed et al., 2022) and distill algorithms (Laskin et al., 2022) for better generalization.

Besides these methods, a promising approach is to utilize representation learning techniques (Sonar et al., 2021; Roy & Konidaris, 2021; Mazouze et al., 2021; Fan & Li, 2022) for learning robust and task-relevant representations. Also, some researchers introduce model-based techniques to imitate the dynamics for generalizing across different dynamics (Lee et al., 2020; Ball et al., 2021; Lyle et al., 2022).

However, there are few attempts to investigate the mechanism behind policy generalization to unseen environments and its connection to the property of the environment distribution. Ghosh et al. (2021) takes the first step to show that generalization to unseen environments will introduce partial observability, thus Markovian and deterministic policies are no longer optimal here. Moreover, some works also experimentally show that stochastic or non-Markovian policies can perform better generalization than deterministic and Markovian policies (Lee et al., 2020; Ghosh et al., 2021).

However, the expression ability of different hypothesis sets and the connection with the environment distribution are still under-explored, which is crucial to analyze current algorithms and design algorithms with stronger generalization.

2.2. World Models

After Ha & Schmidhuber first propose the concept of world models, which hope to learn the environment for better planning (Hafner et al., 2019b) and policy learning (Hafner et al., 2019a; 2020), this field has attracted generous attention. For example, PlaNet (Hafner et al., 2019b) and Dreamer (Hafner et al., 2019a) utilize Recurrent State Space Model (RSSM) (Hafner et al., 2019b) to model the environment, including visual representation, dynamic transition, and reward function, which markedly improves the sample efficiency of visual robot control tasks (Tassa et al., 2018).

Moreover, DreamerV2 (Hafner et al., 2020) proposes some design choices and extends world models to handle discrete-action tasks like Atari. Then, some fellow-up works focus on reconstruction-free world models, which no longer costs representation capacity to reconstruct task-irrelevant parts, for example, Dreaming (Okada & Taniguchi, 2021) proposes a contrastive term of InfoMax objective, and DreamerPro (Deng et al., 2022) introduces prototypes as a non-contrastive self-supervised term. Some works also propose an array of techniques, like temporal predictive coding (Nguyen et al., 2021), cooperative reconstruction (Fu et al., 2021), Denoised MDP (Wang et al., 2022), to better encode task-relevant information into world models.

Currently, an array of works (Chen et al., 2021; Micheli et al., 2022) introduce transformer (Vaswani et al., 2017) into world models to capture long-term dependence and significantly improve performance. Some works also propose to use world models to extract the features of the environment, by learning from videos (Seo et al., 2022) or exploring from the environment (Sekar et al., 2020; Xu et al., 2022), and then finetune to new tasks by utilizing world models.

However, current world models are designed for the single-task setting and can not directly handle different tasks at the same time without finetuning, which is required for zero-shot generalization to unseen tasks.

3. Task Distribution Relevance

In this part, we first formulate task generalization in RL and then analyze the performance of Markovian policies for handling a distribution of tasks via a novel metric Task Distribution Relevance.

3.1. Preliminary

In this work, we consider the setting with a task distribution \mathcal{T} of MDPs, where each environment owns the same transition and different reward functions. This setting is practical and important since we always hope different agents handle their corresponding tasks and generalize to unseen tasks in a general environment.

More formally, each environment \mathcal{M} sampled from \mathcal{T} can be represented as $\mathcal{M} = (\mathcal{S}, \mathcal{A}, \mathcal{P}, \mathcal{R}_{\mathcal{M}}, \gamma)$. Here \mathcal{S} and \mathcal{A} represent the state and action spaces, respectively. For $\forall (s, a) \in \mathcal{S} \times \mathcal{A}$, $\mathcal{P}(\cdot|s, a)$ is a distribution over \mathcal{S} , representing its dynamic. Furthermore, $\mathcal{R}_{\mathcal{M}}(s, a)$ is the reward function of \mathcal{M} and $\gamma \in (0, 1)$ is the discount factor.

For handling the task distribution, we mainly consider three hypothesis sets of policies: (1) The first class Π_1 represents Markovian policies, i.e., $\Pi_1 = \{\pi|\pi : \mathcal{S} \rightarrow \mathcal{D}(\mathcal{A})\}$, here $\mathcal{D}(\mathcal{A})$ represents a distribution over \mathcal{A} , which is widely used and shown optimal for handling single environment; (2) The second class Π_2 represents \mathcal{S} - \mathcal{A} memorized policies, i.e., $\Pi_2 = \{\pi|\pi : \mathcal{H} \rightarrow \mathcal{D}(\mathcal{A})\}$, here $\mathcal{H} = \cup_{t=1}^{\infty} \mathcal{H}_t$, $\mathcal{H}_t = (\mathcal{S} \times \mathcal{A})^{t-1} \times \mathcal{S}$, which is experimentally used (Lee et al., 2020) for improving the generalization of agents to unseen environments; (3) The third class Π_3 represents \mathcal{S} - \mathcal{A} - \mathcal{R} memorized policies, i.e., $\Pi_3 = \{\pi|\pi : \mathcal{I} \rightarrow \mathcal{D}(\mathcal{A})\}$, here $\mathcal{I} = \cup_{t=1}^{\infty} \mathcal{I}_t$, $\mathcal{I}_t = (\mathcal{S} \times \mathcal{A} \times \mathbb{R})^{t-1} \times \mathcal{S}$. We propose encoding reward information into policies here for distinguishing different tasks and further generalizing to unseen tasks.

Naturally we have $\Pi_1 \subseteq \Pi_2 \subseteq \Pi_3$, as shown in Fig. 1. Given the policy $\pi \in \Pi_3$, at each timestep t , the agent will use the history information $(s_0, a_0, r_0, s_1, a_1, r_1, \dots, s_t)$ to sample action a_t , arrive at the next state $s_{t+1} \sim \mathcal{P}(\cdot|s_t, a_t)$, and get the current return $r_t = \mathcal{R}_{\mathcal{M}}(s_t, a_t)$. The performance of policy π in \mathcal{M} is defined as the expectation of the discounted return of the trajectory τ :

$$J_{\mathcal{M}}(\pi) = \mathbb{E}_{\tau \sim \pi} \left[R(\tau) \triangleq \sum_{t=0}^{\infty} \gamma^t r_t \right], \quad (1)$$

where $R(\tau)$ represents the discounted return of τ . In task distribution \mathcal{T} , we hope to find the optimal policy over all tasks sampled from \mathcal{T} , i.e., $\max_{\pi} \mathbb{E}_{\mathcal{M} \sim \mathcal{T}} J_{\mathcal{M}}(\pi)$.

When considering the generalization of agents, some previous work (Ghosh et al., 2021) has shown that the fully-observed environment will be partially observable and Markovian policies set Π_1 , which is optimal when handling

the single task, is no longer optimal. Also, Some work (Lee et al., 2020) empirically finds that encoding historical states and actions into the policy, i.e., using the hypothesis set Π_2 , can gain better generalization than Markovian policies since Π_2 can handle partial observability to some extent.

However, the performance of Π_1, Π_2 and its connection with the task distribution \mathcal{T} are still under-explored without effective metrics of \mathcal{T} , which are studied in the next part.

3.2. Theoretical Analyses

First, we show that, although $\Pi_1 \subseteq \Pi_2$, their expressive abilities are the same, i.e., the optimal return of these two hypothesis sets are the same, and they are both sub-optimal.

Theorem 3.1 (Sub-Optimality of Π_1, Π_2 , Proof in Appendix B.1). *Set $\mathcal{M} = (\mathcal{S}, \mathcal{A}, \mathcal{P}, \mathcal{R}_{\mathcal{M}}, \gamma) \sim \mathcal{T}$. For $\forall \pi \in \Pi_2$, we have $\mathbb{E}_{\mathcal{M} \sim \mathcal{T}} J_{\mathcal{M}}(\pi) = J_{\bar{\mathcal{M}}}(\pi)$, here $\bar{\mathcal{M}} = (\mathcal{S}, \mathcal{A}, \mathcal{P}, \bar{\mathcal{R}}, \gamma)$ and $\bar{\mathcal{R}} = \mathbb{E}_{\mathcal{M} \sim \mathcal{T}}[\mathcal{R}_{\mathcal{M}}]$. Moreover, we have*

$$\begin{aligned} \max_{\pi \in \Pi_2} \mathbb{E}_{\mathcal{M} \sim \mathcal{T}} J_{\mathcal{M}}(\pi) &= \max_{\pi \in \Pi_1} \mathbb{E}_{\mathcal{M} \sim \mathcal{T}} J_{\mathcal{M}}(\pi) \\ &\leq \mathbb{E}_{\mathcal{M} \sim \mathcal{T}} \max_{\pi \in \Pi_1} J_{\mathcal{M}}, \end{aligned} \quad (2)$$

As shown in Theorem 3.1, the cumulative returns of policies in Π_1 and Π_2 are the same as their returns in the ‘‘average’’ MDP $\bar{\mathcal{M}}$, where the reward function is the average of reward functions in different tasks, and they are both sub-optimal. This is because policies in Π_1 and Π_2 choose actions via using current state or historical state-action pairs, which are the same in all tasks, and can not distinguish different tasks. Since we focus on the generalization of different tasks with different reward functions, we propose encoding historical reward signals into policies, i.e., using policies in Π_3 .

Specifically, to investigate the gap between the performance of policies in (Π_1, Π_2) and the optimal return, we propose a novel metric named Task Distribution Relevance (TDR) of the distribution \mathcal{T} as

Definition 3.2 (Task Distribution Relevance). For any task distribution \mathcal{T} and state s , the Task Distribution Relevance of \mathcal{T} and s is defined as

$$\begin{aligned} D_{\text{TDR}}(\mathcal{T}, s) &= \mathbb{E}_{\mathcal{M} \sim \mathcal{T}} [\max_a Q_{\mathcal{M}}^*(s, a)] \\ &\quad - \max_a \mathbb{E}_{\mathcal{M} \sim \mathcal{T}} [Q_{\mathcal{M}}^*(s, a)]. \end{aligned} \quad (3)$$

As shown in Def. 3.2, TDR aims at describing the relevance of \mathcal{T} by using optimal Q functions, which determine the distribution of optimal actions in corresponding tasks. Based on TDR, we can provide a bound of the gap as

Theorem 3.3 (Proof in Appendix B.2). *Assume $\pi_{\mathcal{M}}^* = \arg \max_{\pi} J_{\mathcal{M}}(\pi)$, we have*

$$\begin{aligned} \forall \pi \in \Pi_1 : \mathbb{E}_{\mathcal{M} \sim \mathcal{T}} [J_{\mathcal{M}}(\pi_{\mathcal{M}}^*) - J_{\mathcal{M}}(\pi)] \\ \geq \frac{1}{1 - \gamma} \mathbb{E}_{s \sim d_{\mathcal{M}, \pi}} [D_{\text{TDR}}(\mathcal{T}, s)]. \end{aligned} \quad (4)$$

Set $\pi^* = \arg \max_{\pi \in \Pi_1} J_{\bar{\mathcal{M}}}(\pi)$, we have

$$\begin{aligned} \mathbb{E}_{\mathcal{M} \sim \mathcal{T}} \max_{\pi \in \Pi_1} J_{\mathcal{M}}(\pi) - \max_{\pi \in \Pi_1} \mathbb{E}_{\mathcal{M} \sim \mathcal{T}} J_{\mathcal{M}}(\pi) \\ \geq \frac{1}{1 - \gamma} \mathbb{E}_{s \sim d_{\mathcal{M}, \pi^*}} [D_{\text{TDR}}(\mathcal{T}, s)]. \end{aligned} \quad (5)$$

By Theorem 3.3, we have shown that the performance of hypothesis sets Π_1, Π_2 is related to the TDR of \mathcal{T} . When considering \mathcal{T} with high TDR, i.e., the optimal Q values in different tasks differ greatly, the performance of Π_1 and Π_2 will be extremely poor, since they can not distinguish different tasks and their expressive abilities are significantly limited, which is also shown experimentally in Sec. 5.

4. Methodology

4.1. Reward-Informed World Models

As shown in Theorem 3.1 and Theorem 3.3, policy sets Π_1, Π_2 can not distinguish different tasks with the same dynamic, yielding poor performance in task generalization, especially for the task distribution with high TDR. For distinguishing different tasks, we present to encode reward signals into policies, i.e., using the hypothesis set Π_3 . Moreover, borrowing ideas of Dreamer-oriented world models (Ha & Schmidhuber, 2018; Hafner et al., 2019a), which can capture invariant latent features (Sekar et al., 2020; Xu et al., 2022) for improving the generalization but only fit the single-task setting, we extend it into the task distribution setting with the reward-informed hypothesis set Π_3 and propose our reward-informed world models.

Dreamer (Hafner et al., 2019a) is a visual-based model-based RL method by training world models and parameterized policies. For constructing world models, Dreamer follows Recurrent State Space Model (RSSM) (Hafner et al., 2019b) with the following components:

Deterministic State Model: $h_t = f(h_{t-1}, s_{t-1}, a_{t-1})$,

Transition Model: $p_{\theta}(s_t | h_t)$,

Observation Model: $p_{\theta}(o_t | h_t, s_t)$,

Reward Model: $p_{\theta}(r_t | h_t, s_t)$,

in which the Deterministic State Model encodes historical states and actions into the current hidden feature, then Transition Model, Observation Model, and Reward Model further predict the state, observation, and reward respectively.

Obviously, RSSM is designed for handling the single-task setting and can not handle different tasks, which degenerates the generalization accordingly. To address this issue, we propose novel reward-informed world models which encode the reward signals into the hidden feature. In particular, we design the probabilistic graphical model for analyzing

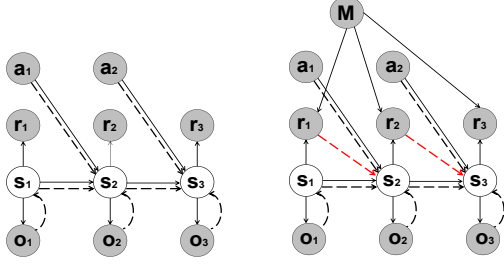


Figure 2. Probabilistic graphical model designs. We represent stochastic variables via circles. Solid and dashed lines represent the generative process and the inference model respectively. The left model represents the single-task situation, where the inference model is usually chosen as $q(s_t|s_{t-1}, a_{t-1}, o_t)$ (Hafner et al., 2019b). The right model represents the task-distribution situation. Since the reward here is also related to the task, we choose our inference model as $q(s_t|s_{t-1}, a_{t-1}, r_{t-1}, o_t)$ to encode rewards.

task-distribution setting in Fig. 2, where the reward does not only rely on the previous state and action, but also on the current task. Thus we can calculate the joint distribution as

$$\begin{aligned} & p(s_{1:T}, o_{1:T}, r_{1:T}, a_{1:T-1}, \mathcal{M}) \\ &= p(\mathcal{M}) \prod_{t=1}^T p(s_{t+1}|s_t, a_t) p(o_t|s_t) p(r_t|s_t, \mathcal{M}), \end{aligned} \quad (6)$$

and further define the reward-informed inference model to encode reward signals and approximate state posteriors as

$$q(s_{1:T}|o_{1:T}, a_{1:T}, r_{1:T}) = \prod_{t=1}^T q(s_t|s_{t-1}, a_{t-1}, r_{t-1}, o_t). \quad (7)$$

Inspired by previous work (Hafner et al., 2019b), we further use reward-informed world models to construct the variational lower bound of the log-likelihood on the data as

$$\begin{aligned} & \ln p(o_{1:T}, r_{1:T}, \mathcal{M}|a_{1:T}) \\ & \geq \sum_{t=1}^T \mathbb{E}_q \ln p(o_t, r_t | \mathcal{M}, s_t) \\ & - \sum_{t=1}^T \mathbb{E}_q \text{KL}(q(s_t|o_{\leq t}, r_{< t}, a_{< t}) || p(s_t|s_{t-1}, a_{t-1})) \\ & + \mathbb{E}_q \ln p(\mathcal{M}|s_{1:T}) \\ & + \mathbb{E}_q \ln \frac{p(o_{1:T}, r_{1:T} | \mathcal{M}, s_{1:T})}{p(o_{1:T}, r_{1:T} | s_{1:T})}. \end{aligned} \quad (8)$$

The detailed proof is provided in Appendix B.3. Here the first two terms in the lower bound are for reconstructing observations, predicting rewards, and inferring states, while the last two terms are for predicting the current task from historical information. Consequently, the last two terms are beneficial for improving the generalization since they help to encode the task information into states.

Algorithm 1 Reward Informed Dreamer (RID)

Require: M training tasks $\{\mathcal{M}_m\}_{m=1}^M$, M replay buffers $\{\mathcal{D}_m\}_{m=1}^M$, N testing tasks $\{\mathcal{M}_{M+n}\}_{n=1}^N$, initialize parameters of world models, the policy, and the critic.

- 1: **while** not converge **do**
- 2: **for** update step = 1, 2, ..., U **do**
- 3: Sample o - a - r pairs $\{(o_t^i, a_t^i, r_t^i)\}_{t=k}^{k+L}$ from each replay buffer $\mathcal{D}_i, i = 1, 2, \dots, M$
- 4: Calculate the deterministic state h via Eq. (10) and further calculate model states s .
- 5: Update the world models via optimizing Eq. (11).
- 6: Collect imagined trajectories from each s via the policy and the world models and use these imagined trajectories to update the policy and the critic.
- 7: **end for**
- 8: Collect trajectories from the environment $\mathcal{M}_m (m = 1, 2, \dots, M)$ and store them into the replay buffer \mathcal{D}_m .
- 9: **end while**
- 10: Evaluate the agent in testing environments $\mathcal{M}_{M+n} (n = 1, 2, \dots, N)$.

4.2. Reward Informed Dreamer

Based on previous analyses, we propose our novel method of Reward Informed Dreamer (RID), which learns from an array of tasks and generalizes to unseen tasks by utilizing reward signals. A brief pseudo code of RID is provided in Algorithm 1, of which the detailed version is in Appendix A.

Given the task distribution \mathcal{T} , we sample M training tasks $\{\mathcal{M}_m\}_{m=1}^M$ from \mathcal{T} for optimizing the agent and hope it can generalize to N unseen testing tasks $\{\mathcal{M}_{M+n}\}_{n=1}^N$ sampled from \mathcal{T} . And the goal of RID is to maximize the expected performance over the distribution \mathcal{T} :

$$\max_{\pi} \mathbb{E}_{\mathcal{M} \sim \mathcal{T}} J_{\mathcal{M}}(\pi). \quad (9)$$

Since the distribution is unknown and hard to calculate, we train our agent in training tasks, i.e., maximizing $\frac{1}{M} \sum_{m=1}^M J_{\mathcal{M}_m}(\pi)$ and evaluate it in testing tasks, i.e., evaluating $\frac{1}{N} \sum_{n=1}^N J_{\mathcal{M}_{M+n}}(\pi)$.

Now we introduce the training of RID in detail. For training reward-informed world models, RID extends RSSM (Hafner et al., 2019b) and encodes all historical information to the deterministic state h by using gated recurrent unit (GRU) (Cho et al., 2014; Chung et al., 2014) as

$$h_t = \text{GRU}(h_{t-1}, s_{t-1}, a_{t-1}, r_{t-1}), \quad (10)$$

which can be easily extended to other architectures like Transformer (Vaswani et al., 2017). Then reward-informed world models will predict the current state, observation, reward, and which task we are handling by $p_{\theta}(s_t|h_t), p_{\theta}(o_t|s_t, h_t), p_{\theta}(r_t|h_t, s_t)$, and $p_{\theta}(\mathcal{M}|s_{1:T})$.

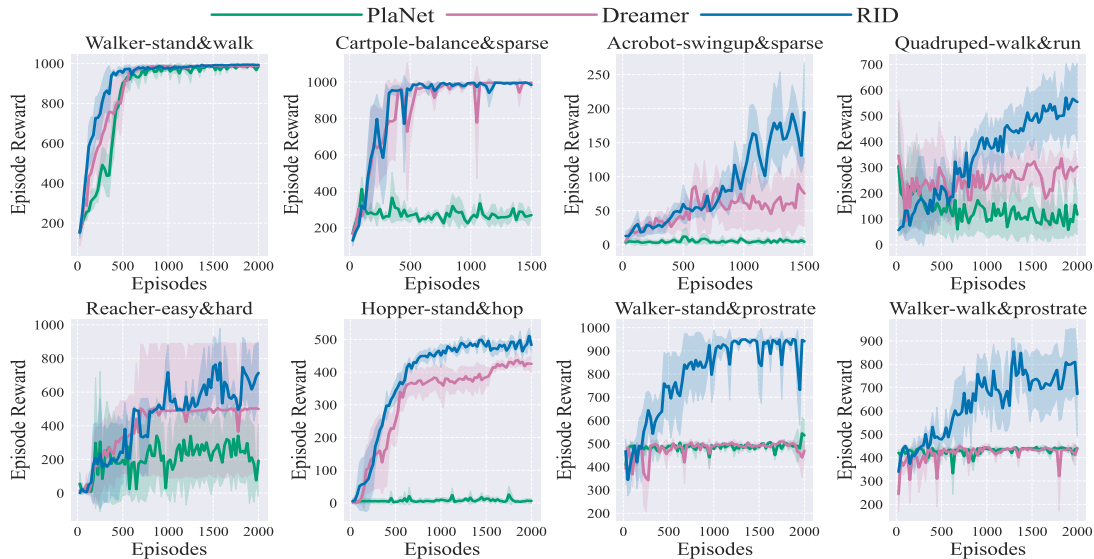


Figure 3. Average cumulative reward curves over different tasks for PlaNet, Dreamer, and RID. The x-axes indicate the number of episodes interacting with the environment, and the y-axes indicate the performance of the agent, including average rewards with standard deviations.

Moreover, we also use a parameterized neural network $\pi_{\theta}(\cdot|h_t, s_t)$ as our policy. In the stage of collecting data, RID will use different replay buffers $\mathcal{D}_1, \mathcal{D}_2, \dots, \mathcal{D}_M$ to store data from $\mathcal{M}_1, \mathcal{M}_2, \dots, \mathcal{M}_M$ respectively. Then in the training stage, RID will sample from each replay buffer and the training objective of the reward-informed world models in our RID is followed Eq. (8) as

$$L_{\text{RID}} = \sum_{i=1}^M \mathbb{E}_q \left[\sum_{t=1}^T \ln p_{\theta}(o_t^i | h_t^i, s_t^i) + \sum_{t=1}^T \ln p_{\theta}(r_t^i | h_t^i, s_t^i) - \sum_{t=1}^T D_{\text{KL}}(q(s_t^i | h_t^i, o_t^i) \| p_{\theta}(s_t^i | h_t^i)) + \ln p_{\theta}(\mathcal{M}_i | s_{1:T}^i) \right]. \quad (11)$$

Here the first three items in Eq. (11) are similar to Dreamer for reconstructing observations, predicting rewards, and inferring states. The novel last term in Eq. (11) is calculated in Eq. (8) for encouraging the agent to encode task information into hidden states and infer the current task via these hidden states, which is beneficial for generalizing to unseen tasks.

As for training the actor-critic, which are both parameterized neural networks, we follow the actor-critic policy learning in Dreamer (Hafner et al., 2019a) with a more powerful hypothesis set Π_3 , which encodes reward signals into policies and further uses states to predict the task for improving the generalization. When optimizing the policy, RID samples an array of states from the replay buffer and starts from them to imagine trajectories via interacting with reward-informed world models, which is fixed at this time. Here the reward-informed world models can capture the invariant features, which are beneficial for the agent to train more effectively and gain better generalization. After getting imagined tra-

jectories, the agent can be optimized via maximizing the λ -return (Schulman et al., 2015) and the critic can be optimized via regressing the targets calculated by the temporal difference algorithm (Sutton & Barto, 2018).

5. Experiments

5.1. Experimental Setup

Environments and Tasks. First, to show the scalability and the superiority of RID and verify analyses about TDR in Sec. 3, we consider an array of different combinations of tasks in DeepMind control suite (Tassa et al., 2018), including (1) four task combinations of **Walker-stand&walk**, **Cartpole-balance&sparse**, **Acrobot-swingup&sparse** and **Quadruped-walk&run**, which share the same optimal actions with TDR being 0; and (2) two task combinations with low TDR of **Reacher-easy&hard** and **Hopper-stand&hop**. We also consider (3) another two task combinations with high TDR of **Walker-stand&prostrate** and **Walker-walk&prostrate**. For example, the Walker-stand task hopes a two-leg robot maintain its height above a certain threshold while the Walker-prostrate hopes the height is below another certain threshold, yielding almost opposite optimal Q functions with huge TDR. More details about these task combinations are in Appendix C.

Moreover, we design some task distributions by extending tasks in DeepMind control suite for evaluating algorithms' generalization. For each task distribution, we will sample some tasks as training tasks and testing tasks respectively. Descriptions of these task distributions are as below and more details are also in Appendix C.

Reward Informed Dreamer

Tasks	Walker-stand&walk	Cartpole-balance&sparse	Acrobot-swingup&sparse	Quadruped-walk&run
PlaNet	990.6 ± 3.8	412.8 ± 65.9	12.2 ± 9.8	305.3 ± 206.6
Dreamer	992.3 ± 1.7	997.1 ± 1.1	89.3 ± 58.0	345.4 ± 218.3
RID	994.6 ± 0.1	997.3 ± 0.7	194.7 ± 72.5	571.2 ± 131.4
Tasks	Reacher-easy&hard	Hopper-stand&hop	Walker-stand&prostrate	Walker-walk&prostrate
PlaNet	341.0 ± 228.3	25.9 ± 25.7	544.3 ± 68.6	445.4 ± 5.1
Dreamer	506.1 ± 382.9	436.9 ± 18.9	510.0 ± 6.7	449.7 ± 12.5
RID	775.2 ± 203.1	510.7 ± 22.8	951.0 ± 2.8	855.3 ± 56.2

Table 1. Average cumulative reward over different tasks (mean ± one std) of the best policy trained by PlaNet, Dreamer, RID in different tasks. Numbers greater than 95 % of the best performance for each tasks are **bold**.

- **Cheetah_speed**(α, β). This task distribution is based on the task Cheetah-run in DeepMind control suite. Tasks here require a running planar biped to run within the target speed interval ($\alpha - \beta, \alpha + \beta$). We train the agents in tasks with parameters (0.5, 0.2), (1.5, 0.2), (2.0, 0.2), (3.0, 0.2) and test them in tasks with parameters (1.0, 0.2), (2, 5, 0.2).
- **Pendulum_angle**(α, β). This task distribution is based on the task Pendulum-swingup in DeepMind control suite. Tasks here hope an inverted pendulum stay its pole within the target angle interval ($\arccos \alpha, \arccos \beta$). Training tasks are with parameters (-0.95, -0.9), (-0.85, -0.8), (-0.8, -0.75), (-0.7, -0.65) and testing tasks are with parameters (-0.9, -0.85), (-0, 75, -0.7).
- **Quadruped_speed**(α, β). This task distribution is based on the task Quadruped-run in DeepMind control suite. Tasks here require a quadruped agent to run within the target speed interval ($\alpha - \beta, \alpha + \beta$). We train the agents in tasks with parameters (0.5, 0.2), (1.5, 0.2), (2.0, 0.2), (3.0, 0.2) and test in tasks with parameters (1.0, 0.2), (2, 5, 0.2).

Baselines and Evaluation Metrics. We compare RID with two classic world models PlaNet (Hafner et al., 2019b) and Dreamer (Hafner et al., 2019a), which both utilize all historical state-actions for taking the current action and belong to Π_2 . For the multi-task setting, we evaluate the average return of all tasks. For the task generalization setting, we train agents in all training tasks and evaluate them in both training and testing tasks. For all experiments, we train 3 policies with different random seeds and calculate the mean and standard deviations to mitigate the effects of randomness caused by stochastic environments and policies.

5.2. Experimental Results for TDR

We first report the results of the multi-task setting for verifying our analyses about TDR and showing the effectiveness of RID. We plot the mean and standard deviations of returns

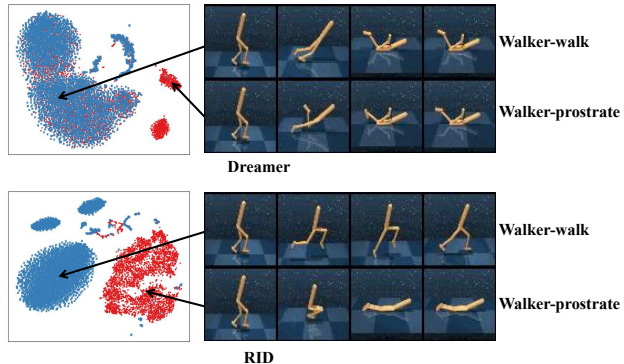


Figure 4. Visualization of Dreamer and RID for handling Walker-walk&Prostrate. The upper subfigure and the below subfigure represent the result of Dreamer and RID respectively. For each algorithm in each task, we show the observation of 4 frames of a trajectory in the right part of the subfigure. In the left part of each subfigure, we draw the t-SNE (Van der Maaten & Hinton, 2008) result of all states in trajectories of two tasks, where blue points and red points represent states in Walker-walk and Walker-prostrate respectively. We also provide videos of these trajectories in the supplementary materials.

as functions of the episode number in the training stage in Fig. 3, where the solid line and the lighter part represent the mean and standard deviations respectively. Also, we report the optimal mean ± standard deviations of the average cumulative return of all environments in Table 1.

As shown in Table 1 and Fig. 3, RID outperforms baselines in all environments, especially in those with high TDR. In tasks of which the TDR is 0, like Walker-stand&walk and Cartpole-balance&sparse, the optimal performance of RID and baselines are similar since these tasks share the same optimal action and Π_1, Π_2 own the optimal policy at this case, which is derived in Theorem 3.3. In these cases, our RID can still converge faster and show more robust performance. In Acrobot-swingup&sparse and Quadruped-walk&run, although the TDR of these tasks is 0, RID can outperform baselines since it can better distinguish different tasks. Finally, in the last four environments with non-zero TDR, RID achieves a remarkable improvement compared with baselines. Especially, in Walker-stand&prostrate and

Tasks	Cheetah_speed		Pendulum_angle		Quadruped_speed	
	Train	Test	Train	Test	Train	Test
PlaNet	176.6 ± 25.9	83.0 ± 52.2	99.8 ± 28.3	80.5 ± 24.2	24.8 ± 17.5	7.9 ± 5.8
Dreamer	250.2 ± 9.6	3.0 ± 2.2	92.2 ± 19.9	79.6 ± 14.8	28.3 ± 1.1	20.1 ± 1.0
RID	956.8 ± 6.0	787.4 ± 163.6	287.3 ± 22.8	126.6 ± 31.8	37.6 ± 3.1	39.6 ± 3.0

Table 2. Average cumulative reward over different tasks (mean ± one std) of the best policy trained by PlaNet, Dreamer, and RID in different tasks. For each task distribution, we train agents in the train tasks and evaluate them in both train and test environments. Numbers greater than 95 percent of the best performance for each environment are **bold**.

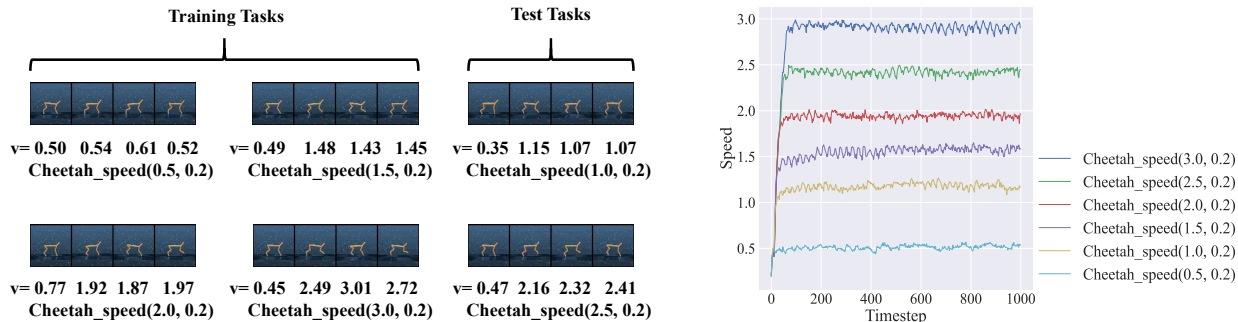


Figure 5. Visualization of the trained RID agent in the task distribution of Cheetah_speed. In the left part, the left four subfigures and the right two subfigures show the results of train and test tasks respectively. For each task, we show the observation and its corresponding speed of 4 timesteps in a trajectory. In the right part, we plot the speed of the agent as a function of timesteps in all tasks. We also provide videos of these trajectories in the supplementary materials.

Walker-walk&prostrate, of which the TDR is significantly huge, baselines can not effectively train the agent since these policies belong to Π_2 and can not distinguish different tasks, which still matches our Theorem 3.3, while RID can distinguish them by utilizing reward signals and improves the performance conspicuously.

Moreover, to better show that RID can encode task information into states and further handle different tasks without extra task knowledge, we sample trajectories of the trained agent via Dreamer as well as RID in Walker-walk&prostrate and visualize some observations as well as all states, of which the dimensions are reduced for visualization by t-SNE (Van der Maaten & Hinton, 2008). As shown in Fig. 4, Dreamer can not distinguish different tasks and perform the same in different tasks, while our RID can distinguish them and perform correct actions in corresponding tasks. Also, states of different tasks in Dreamer are mixed, while in RID, states of different tasks can be distinguished since they encode the task information.

5.3. Experimental Results for Task Generalization

Furthermore, we report the results of the task generalization setting to show that our RID can effectively generalize the policy to unseen tasks via encoding the reward information. In Table 2, we report the optimal result of training tasks as well as test tasks in environments mentioned in Sec. 5.1. As shown in Table 2, compared with baselines, our RID can significantly improve the average cumulative return in both

training tasks and testing tasks, which shows that RID can both handle multiple training tasks at the same time and generalize to unseen testing tasks effectively.

Finally, for agents trained by RID in the task distribution Cheetah_speed, we visualize several observations with their corresponding speeds of all tasks, including training ones and testing ones and the speed curve of the whole trajectory, in Fig. 5. As shown here, RID can successfully distinguish different tasks via reward signals and make the agent reach the target speed, even in testing tasks with which the agent has not interacted in the training stage.

6. Conclusion

In this work, we propose a novel metric Task Distribution Relevance (TDR) to capture the relevance of the task distribution and show that Markovian policies will perform poorly in tasks with high TDR. Moreover, for improving generalization over tasks, we propose a novel framework of Reward Informed Dreamer (RID) which encodes reward signals into policies for distinguishing different tasks and utilizes novel reward-informed world models to capture invariant latent features. In RID, we calculate the corresponding variational lower bound of the log-likelihood on data, which includes a novel loss term to distinguish different tasks via states. Experimental results in DeepMind control demonstrate that RID can remarkably improve the performance of handling different tasks at the same time, especially for high TDR ones, and successfully generalize to unseen tasks.

References

- Ball, P. J., Lu, C., Parker-Holder, J., and Roberts, S. Augmented world models facilitate zero-shot dynamics generalization from a single offline environment. In *International Conference on Machine Learning*, pp. 619–629. PMLR, 2021.
- Chen, C., Yoon, J., Wu, Y.-F., and Ahn, S. Transdreamer: Reinforcement learning with transformer world models. In *Deep RL Workshop NeurIPS 2021*, 2021.
- Cho, K., van Merriënboer, B., Bahdanau, D., and Bengio, Y. On the properties of neural machine translation: Encoder-decoder approaches. In *8th Workshop on Syntax, Semantics and Structure in Statistical Translation, SSST 2014*, pp. 103–111. Association for Computational Linguistics (ACL), 2014.
- Chung, J., Gulcehre, C., Cho, K., and Bengio, Y. Empirical evaluation of gated recurrent neural networks on sequence modeling. *arXiv preprint arXiv:1412.3555*, 2014.
- Cobbe, K., Klimov, O., Hesse, C., Kim, T., and Schulman, J. Quantifying generalization in reinforcement learning. In *International Conference on Machine Learning*, pp. 1282–1289. PMLR, 2019.
- Deng, F., Jang, I., and Ahn, S. Dreamerpro: Reconstruction-free model-based reinforcement learning with prototypical representations. In *International Conference on Machine Learning*, pp. 4956–4975. PMLR, 2022.
- Fan, J. and Li, W. Dribo: Robust deep reinforcement learning via multi-view information bottleneck. In *International Conference on Machine Learning*, pp. 6074–6102. PMLR, 2022.
- Fu, X., Yang, G., Agrawal, P., and Jaakkola, T. Learning task informed abstractions. In *International Conference on Machine Learning*, pp. 3480–3491. PMLR, 2021.
- Ghosh, D., Rahme, J., Kumar, A., Zhang, A., Adams, R. P., and Levine, S. Why generalization in rl is difficult: Episodic pomdps and implicit partial observability. *Advances in Neural Information Processing Systems*, 34:25502–25515, 2021.
- Ha, D. and Schmidhuber, J. World models. *arXiv preprint arXiv:1803.10122*, 2018.
- Hafner, D., Lillicrap, T., Ba, J., and Norouzi, M. Dream to control: Learning behaviors by latent imagination. In *International Conference on Learning Representations*, 2019a.
- Hafner, D., Lillicrap, T., Fischer, I., Villegas, R., Ha, D., Lee, H., and Davidson, J. Learning latent dynamics for planning from pixels. In *International conference on machine learning*, pp. 2555–2565. PMLR, 2019b.
- Hafner, D., Lillicrap, T. P., Norouzi, M., and Ba, J. Mastering atari with discrete world models. In *International Conference on Learning Representations*, 2020.
- Hansen, N. and Wang, X. Generalization in reinforcement learning by soft data augmentation. In *2021 IEEE International Conference on Robotics and Automation (ICRA)*, pp. 13611–13617. IEEE, 2021.
- Igl, M., Ciosek, K., Li, Y., Tschitschek, S., Zhang, C., Devlin, S., and Hofmann, K. Generalization in reinforcement learning with selective noise injection and information bottleneck. *Advances in neural information processing systems*, 32, 2019.
- Kakade, S. and Langford, J. Approximately optimal approximate reinforcement learning. In *In Proc. 19th International Conference on Machine Learning (ICML)*. Citeseer, 2002.
- Kendall, A., Hawke, J., Janz, D., Mazur, P., Reda, D., Allen, J.-M., Lam, V.-D., Bewley, A., and Shah, A. Learning to drive in a day. In *2019 International Conference on Robotics and Automation (ICRA)*, pp. 8248–8254. IEEE, 2019.
- Kirk, R., Zhang, A., Grefenstette, E., and Rocktäschel, T. A survey of generalisation in deep reinforcement learning. *arXiv preprint arXiv:2111.09794*, 2021.
- Laskin, M., Wang, L., Oh, J., Parisotto, E., Spencer, S., Steigerwald, R., Strouse, D., Hansen, S., Filos, A., Brooks, E., et al. In-context reinforcement learning with algorithm distillation. *arXiv preprint arXiv:2210.14215*, 2022.
- Lee, K., Lee, K., Shin, J., and Lee, H. Network randomization: A simple technique for generalization in deep reinforcement learning. In *International Conference on Learning Representations*, 2019.
- Lee, K., Seo, Y., Lee, S., Lee, H., and Shin, J. Context-aware dynamics model for generalization in model-based reinforcement learning. In *International Conference on Machine Learning*, pp. 5757–5766. PMLR, 2020.
- Lyle, C., Rowland, M., Dabney, W., Kwiatkowska, M., and Gal, Y. Learning dynamics and generalization in reinforcement learning. *arXiv preprint arXiv:2206.02126*, 2022.
- Mazouze, B., Ahmed, A. M., Hjelm, R. D., Kolobov, A., and MacAlpine, P. Cross-trajectory representation learning for zero-shot generalization in rl. In *International Conference on Learning Representations*, 2021.
- Micheli, V., Alonso, E., and Fleuret, F. Transformers are sample-efficient world models. In *Deep Reinforcement Learning Workshop NeurIPS 2022*, 2022.

- Mnih, V., Kavukcuoglu, K., Silver, D., Rusu, A. A., Veness, J., Bellemare, M. G., Graves, A., Riedmiller, M. A., Fidjeland, A., Ostrovski, G., Petersen, S., Beattie, C., Sadik, A., Antonoglou, I., King, H., Kumaran, D., Wierstra, D., Legg, S., and Hassabis, D. Human-level control through deep reinforcement learning. *Nature*, 518 (7540):529–533, 2015. URL <https://doi.org/10.1038/nature14236>.
- Nguyen, T. D., Shu, R., Pham, T., Bui, H., and Ermon, S. Temporal predictive coding for model-based planning in latent space. In *International Conference on Machine Learning*, pp. 8130–8139. PMLR, 2021.
- Okada, M. and Taniguchi, T. Dreaming: Model-based reinforcement learning by latent imagination without reconstruction. In *2021 IEEE International Conference on Robotics and Automation (ICRA)*, pp. 4209–4215. IEEE, 2021.
- Raileanu, R. and Fergus, R. Decoupling value and policy for generalization in reinforcement learning. In *International Conference on Machine Learning*, pp. 8787–8798. PMLR, 2021.
- Raileanu, R., Goldstein, M., Yarats, D., Kostrikov, I., and Fergus, R. Automatic data augmentation for generalization in reinforcement learning. *Advances in Neural Information Processing Systems*, 34:5402–5415, 2021.
- Reed, S., Zolna, K., Parisotto, E., Colmenarejo, S. G., Novikov, A., Barth-Maron, G., Gimenez, M., Sulsky, Y., Kay, J., Springenberg, J. T., et al. A generalist agent. *arXiv preprint arXiv:2205.06175*, 2022.
- Roy, J. and Konidaris, G. D. Visual transfer for reinforcement learning via wasserstein domain confusion. In *Proceedings of the AAAI Conference on Artificial Intelligence*, volume 35, pp. 9454–9462, 2021.
- Schulman, J., Moritz, P., Levine, S., Jordan, M., and Abbeel, P. High-dimensional continuous control using generalized advantage estimation. *arXiv preprint arXiv:1506.02438*, 2015.
- Sekar, R., Rybkin, O., Daniilidis, K., Abbeel, P., Hafner, D., and Pathak, D. Planning to explore via self-supervised world models. In *International Conference on Machine Learning*, pp. 8583–8592. PMLR, 2020.
- Seo, Y., Lee, K., James, S. L., and Abbeel, P. Reinforcement learning with action-free pre-training from videos. In *International Conference on Machine Learning*, pp. 19561–19579. PMLR, 2022.
- Silver, D., Huang, A., Maddison, C. J., Guez, A., Sifre, L., van den Driessche, G., Schrittwieser, J., Antonoglou, I., Panneershelvam, V., Lanctot, M., Dieleman, S., Grewe, D., Nham, J., Kalchbrenner, N., Sutskever, I., Lillicrap, T. P., Leach, M., Kavukcuoglu, K., Graepel, T., and Hassabis, D. Mastering the game of go with deep neural networks and tree search. *Nature*, 529(7587):484–489, 2016. URL <https://doi.org/10.1038/nature16961>.
- Sonar, A., Pacelli, V., and Majumdar, A. Invariant policy optimization: Towards stronger generalization in reinforcement learning. In *Learning for Dynamics and Control*, pp. 21–33. PMLR, 2021.
- Song, X., Jiang, Y., Tu, S., Du, Y., and Neyshabur, B. Observational overfitting in reinforcement learning. In *International Conference on Learning Representations*, 2019.
- Sutton, R. S. and Barto, A. G. *Reinforcement learning: An introduction*. MIT press, 2018.
- Tassa, Y., Doron, Y., Muldal, A., Erez, T., Li, Y., Casas, D. d. L., Budden, D., Abdolmaleki, A., Merel, J., Lefrancq, A., et al. Deepmind control suite. *arXiv preprint arXiv:1801.00690*, 2018.
- Van der Maaten, L. and Hinton, G. Visualizing data using t-sne. *Journal of machine learning research*, 9(11), 2008.
- Vaswani, A., Shazeer, N., Parmar, N., Uszkoreit, J., Jones, L., Gomez, A. N., Kaiser, L., and Polosukhin, I. Attention is all you need. *Advances in neural information processing systems*, 30, 2017.
- Wang, K., Kang, B., Shao, J., and Feng, J. Improving generalization in reinforcement learning with mixture regularization. *Advances in Neural Information Processing Systems*, 33:7968–7978, 2020.
- Wang, T., Du, S., Torralba, A., Isola, P., Zhang, A., and Tian, Y. Denoised mdps: Learning world models better than the world itself. In *International Conference on Machine Learning*, pp. 22591–22612. PMLR, 2022.
- Xu, Y., Parker-Holder, J., Pacchiano, A., Ball, P. J., Rybkin, O., Roberts, S. J., Rocktäschel, T., and Grefenstette, E. Learning general world models in a handful of reward-free deployments. *arXiv preprint arXiv:2210.12719*, 2022.
- Ying, C., Zhou, X., Su, H., Yan, D., Chen, N., and Zhu, J. Towards safe reinforcement learning via constraining conditional value-at-risk. *arXiv preprint arXiv:2206.04436*, 2022.
- Zhang, C., Vinyals, O., Munos, R., and Bengio, S. A study on overfitting in deep reinforcement learning. *arXiv preprint arXiv:1804.06893*, 2018.
- Zhao, C., Sigaud, O., Stulp, F., and Hospedales, T. M. Investigating generalisation in continuous deep reinforcement learning. *arXiv preprint arXiv:1902.07015*, 2019.

A. Pseudo Code of RID

Algorithm 2 Reward Informed Dreamer (RID)

Require: M training tasks $\{\mathcal{M}_m\}_{m=1}^M$, M replay buffers $\{\mathcal{D}_m\}_{m=1}^M$, N testing tasks $\{\mathcal{M}_{M+n}\}_{n=1}^N$, initialize neural network parameters of world models, the policy, and the critic

- 1: **while** not converge **do**
- 2: // *Model Training*
- 3: **for** update step = 1, 2, ..., U **do**
- 4: Sample observation-action-reward pairs from each replay buffer $\{(o_t^i, a_t^i, r_t^i)_{t=k}^{k+L}\} \sim \mathcal{D}_i, i = 1, 2, \dots, M$
- 5: Calculate the deterministic state h via Eq. (10) and further calculate model states s .
- 6: Update the world models via optimizing Eq. (11).
- 7: Collect imagined trajectories from each s_t via the policy and the world models.
- 8: Use these imagined trajectories to update the policy and the critic.
- 9: **end for**
- 10: // *Data Collection*
- 11: **for** $m = 1, 2, \dots, M$ **do**
- 12: $o_1 \leftarrow \mathcal{M}_m.reset()$
- 13: **for** sample step = 1, 2, ..., S **do**
- 14: Compute h_t, s_t and sample action a_t via the policy.
- 15: $r_t, o_{t+1} \leftarrow \mathcal{M}_m.step(a_t)$
- 16: **end for**
- 17: Add these data to the replay buffer \mathcal{D}_m .
- 18: **end for**
- 19: **end while**
- 20: // *Model Evaluation*
- 21: **for** $n = 1, 2, \dots, N$ **do**
- 22: $o_1 \leftarrow \mathcal{M}_{M+n}.reset()$
- 23: **while** the environment not done **do**
- 24: Compute h_t, s_t and sample action a_t via the policy.
- 25: $r_t, o_{t+1} \leftarrow \mathcal{M}_{M+n}.step(a_t)$
- 26: **end while**
- 27: **end for**

B. Proof of Theorems

In this section, we will provide detailed proofs of theorems in the paper.

B.1. The Proof of Theorem 3.1

Proof. We first prove that for $\forall \pi \in \Pi_2$, we have $\mathbb{E}_{\mathcal{M} \sim \mathcal{T}} J_{\mathcal{M}}(\pi) = J_{\bar{\mathcal{M}}}(\pi)$.

For any $\mathcal{M} = (\mathcal{S}, \mathcal{A}, \mathcal{P}, \mathcal{R}_{\mathcal{M}}, \gamma)$, we can use the policy π to interact with \mathcal{M} and get the trajectory $\tau = (s_0^{\mathcal{M}}, a_0^{\mathcal{M}}, r_1^{\mathcal{M}}, s_1^{\mathcal{M}}, a_1^{\mathcal{M}}, r_2^{\mathcal{M}}, \dots)$. Since the dynamic transition \mathcal{P} is the same for all \mathcal{M} and the policy $\pi \in \Pi_2$ only depends on historical states and actions, we naturally have that the distribution of all states and actions $(s_0^{\mathcal{M}}, a_0^{\mathcal{M}}, s_1^{\mathcal{M}}, a_1^{\mathcal{M}}, \dots)$ are the same for all $\mathcal{M} \sim \mathcal{T}$ as well as $\bar{\mathcal{M}}$. Consequently, we have

$$\begin{aligned}
 \mathbb{E}_{\mathcal{M} \sim \mathcal{T}} J_{\mathcal{M}}(\pi) &= \mathbb{E}_{\mathcal{M} \sim \mathcal{T}} \mathbb{E}_{\tau \sim \mathcal{P}, \pi} R_{\mathcal{M}}(\tau) = \mathbb{E}_{\mathcal{M} \sim \mathcal{T}} \mathbb{E}_{\tau \sim \mathcal{P}, \pi} \left[\sum_{t=0}^{\infty} \gamma^t r_t^{\mathcal{M}} \right] \\
 &= \mathbb{E}_{\tau \sim \mathcal{P}, \pi} \left[\sum_{t=0}^{\infty} \gamma^t \mathbb{E}_{\mathcal{M} \sim \mathcal{T}} [r_t^{\mathcal{M}}] \right] = \mathbb{E}_{\tau \sim \mathcal{P}, \pi} \left[\sum_{t=0}^{\infty} \gamma^t \mathbb{E}_{\mathcal{M} \sim \mathcal{T}} [\mathcal{R}_{\mathcal{M}}(s_t^{\mathcal{M}}, a_t^{\mathcal{M}})] \right] \\
 &= \mathbb{E}_{\tau \sim \mathcal{P}, \pi} \left[\sum_{t=0}^{\infty} \gamma^t [\bar{\mathcal{R}}(s_t^{\mathcal{M}}, a_t^{\mathcal{M}})] \right] = \mathbb{E}_{\tau \sim \mathcal{P}, \pi} R_{\bar{\mathcal{M}}}(\tau) = J_{\bar{\mathcal{M}}}(\pi).
 \end{aligned} \tag{12}$$

It is well known that the optimal policy in single MDP is memory-less, i.e., $\max_{\pi \in \Pi_2} J_{\mathcal{M}}(\pi) = \max_{\pi \in \Pi_1} J_{\mathcal{M}}(\pi)$. Consequently, we have

$$\max_{\pi \in \Pi_2} \mathbb{E}_{\mathcal{M} \sim \mathcal{T}} J_{\mathcal{M}}(\pi) = \max_{\pi \in \Pi_2} J_{\mathcal{M}}(\pi) = \max_{\pi \in \Pi_1} J_{\mathcal{M}}(\pi) = \max_{\pi \in \Pi_1} \mathbb{E}_{\mathcal{M} \sim \mathcal{T}} J_{\mathcal{M}}(\pi) \leq \mathbb{E}_{\mathcal{M} \sim \mathcal{T}} \max_{\pi \in \Pi_1} J_{\mathcal{M}}(\pi). \quad (13)$$

Thus we have proven this result. \square

B.2. The Proof of Theorem 3.3

Proof. Our proof follows some previous work (Kakade & Langford, 2002; Ying et al., 2022). First, we consider the bellman equation of value function of $\pi, \pi_{\mathcal{M}}^* \in \Pi_1$ in \mathcal{M} as

$$\begin{aligned} V_{\mathcal{M}, \pi}(s) &= \sum_a \pi(a|s) \left[\mathcal{R}(s, a) + \gamma \sum_{s'} \mathcal{P}(s'|s, a) V_{\mathcal{M}, \pi}(s') \right], \\ V_{\mathcal{M}, \pi_{\mathcal{M}}^*}(s) &= \sum_a \pi_{\mathcal{M}}^*(a|s) \left[\mathcal{R}(s, a) + \gamma \sum_{s'} \mathcal{P}(s'|s, a) V_{\mathcal{M}, \pi_{\mathcal{M}}^*}(s') \right]. \end{aligned}$$

Defining $\Delta V(s) \triangleq V_{\mathcal{M}, \pi}(s) - V_{\mathcal{M}, \pi_{\mathcal{M}}^*}(s)$ as the difference of these two value functions, we can further deduce that

$$\begin{aligned} \Delta V(s) &= V_{\mathcal{M}, \pi}(s) - V_{\mathcal{M}, \pi_{\mathcal{M}}^*}(s) \\ &= \gamma \sum_a \Delta \pi(a|s) \sum_{s'} \mathcal{P}(s'|s, a) V_{\mathcal{M}, \pi_{\mathcal{M}}^*}(s') + \gamma \sum_a \pi(a|s) \sum_{s'} \mathcal{P}(s'|s, a) \Delta V(s') + \sum_a \Delta \pi(a|s) \mathcal{R}(s, a) \\ &= \sum_a \Delta \pi(a|s) Q_{\mathcal{M}, \pi_{\mathcal{M}}^*}(s, a) + \gamma \sum_a \pi(a|s) \sum_{s'} \mathcal{P}(s'|s, a) \Delta V(s'), \end{aligned} \quad (14)$$

here $\Delta \pi(a|s) = \pi(a|s) - \pi_{\mathcal{M}}^*(a|s)$. Since Eq. (14) holds for any s , thus we calculate its expectation for $s \sim d_{\mathcal{M}}^{\pi_{\mathcal{M}}^*}$:

$$\begin{aligned} \sum_s d_{\mathcal{M}}^{\pi}(s) \Delta V(s) &= \sum_s d_{\mathcal{M}}^{\pi}(s) [V_{\mathcal{M}, \pi}(s) - V_{\mathcal{M}, \pi_{\mathcal{M}}^*}(s)] \\ &= \sum_s d_{\mathcal{M}}^{\pi}(s) \sum_a \Delta \pi(a|s) Q_{\mathcal{M}, \pi_{\mathcal{M}}^*}(s, a) + \gamma \sum_s d_{\mathcal{M}}^{\pi}(s) \sum_a \pi(a|s) \sum_{s'} \mathcal{P}(s'|s, a) \Delta V(s') \\ &= \sum_s d_{\mathcal{M}}^{\pi}(s) \sum_a \Delta \pi(a|s) Q_{\mathcal{M}, \pi_{\mathcal{M}}^*}(s, a) + \sum_{s'} \Delta V(s') \left[\gamma \sum_s d_{\mathcal{M}}^{\pi}(s) \sum_a \pi(a|s) \mathcal{P}(s'|s, a) \right]. \end{aligned} \quad (15)$$

Since $d_{\mathcal{M}}^{\pi}(s) - (1 - \gamma) \mathcal{P}(s_0 = s) = \gamma \sum_{s'} d_{\mathcal{M}}^{\pi}(s') \sum_a \pi(a|s') \mathcal{P}(s|s', a)$, we can further prove that

$$\sum_s d_{\mathcal{M}}^{\pi}(s) \Delta V(s) = \sum_s d_{\mathcal{M}}^{\pi}(s) \sum_a \Delta \pi(a|s) Q_{\mathcal{M}, \pi_{\mathcal{M}}^*}(s, a) + \sum_{s'} \Delta V(s') [d_{\mathcal{M}}^{\pi}(s') - (1 - \gamma) \mathcal{P}(s_0 = s')]. \quad (16)$$

By moving the second term of the right part in Eq. (16) to the left part, we can deduce that

$$(1 - \gamma) \sum_{s'} \Delta V(s') \mathcal{P}(s_0 = s') = \sum_s d_{\mathcal{M}}^{\pi}(s) \sum_a \Delta \pi(a|s) Q_{\mathcal{M}, \pi_{\mathcal{M}}^*}(s, a), \quad (17)$$

thus we can calculate that

$$\begin{aligned} J_{\mathcal{M}}(\pi) - J_{\mathcal{M}}(\pi_{\mathcal{M}}^*) &= \sum_{s'} \Delta V(s') \mathcal{P}(s_0 = s') = \frac{1}{1 - \gamma} \sum_s d_{\mathcal{M}}^{\pi}(s) \sum_a \Delta \pi(a|s) Q_{\mathcal{M}, \pi_{\mathcal{M}}^*}(s, a) \\ &= \frac{1}{1 - \gamma} \sum_s d_{\mathcal{M}}^{\pi}(s) \sum_a [\pi(a|s) - \pi_{\mathcal{M}}^*(a|s)] Q_{\mathcal{M}, \pi_{\mathcal{M}}^*}(s, a) \\ &= \frac{1}{1 - \gamma} \mathbb{E}_{s \sim d_{\mathcal{M}}^{\pi}} \mathbb{E}_{a \sim \pi(\cdot|s)} \left(1 - \frac{\pi_{\mathcal{M}}^*(a|s)}{\pi(a|s)} \right) Q_{\mathcal{M}, \pi_{\mathcal{M}}^*}(s, a) \\ &= \frac{1}{1 - \gamma} \mathbb{E}_{s \sim d_{\mathcal{M}}^{\pi}} \int_{\mathcal{A}} \pi(a|s) \left(1 - \frac{\pi_{\mathcal{M}}^*(a|s)}{\pi(a|s)} \right) Q_{\mathcal{M}}^*(s, a) da \\ &= \frac{1}{1 - \gamma} \mathbb{E}_{s \sim d_{\mathcal{M}}^{\pi}} \left[\int_a \pi(a|s) Q_{\mathcal{M}}^*(s, a) da - \max_a Q_{\mathcal{M}}^*(s, a) \right]. \end{aligned} \quad (18)$$

Consequently, we have

$$\begin{aligned}
 \mathbb{E}_{\mathcal{M} \sim \mathcal{T}} [J_{\mathcal{M}}(\pi_{\mathcal{M}}^*) - J_{\mathcal{M}}(\pi)] &= \frac{1}{1-\gamma} \mathbb{E}_{\mathcal{M} \sim \mathcal{T}} \mathbb{E}_{s \sim d_{\mathcal{M}, \pi}(\cdot)} \left[\max_a Q_{\mathcal{M}}^*(s, a) - \int_a \pi(a|s) Q_{\mathcal{M}}^*(s, a) da \right] \\
 &\geq \frac{1}{1-\gamma} \mathbb{E}_{s \sim d_{\mathcal{M}, \pi}(\cdot)} \left[\mathbb{E}_{\mathcal{M} \sim \mathcal{T}} \max_a Q_{\mathcal{M}}^*(s, a) - \max_a \mathbb{E}_{\mathcal{M} \sim \mathcal{T}} Q_{\mathcal{M}}^*(s, a) \right] \\
 &= \frac{1}{1-\gamma} \mathbb{E}_{s \sim d_{\mathcal{M}, \pi}} [D_{\text{TDR}}(\mathcal{T}, s)].
 \end{aligned} \tag{19}$$

Since $J_{\mathcal{M}}(\pi_{\mathcal{M}}^*) = \max_{\pi \in \Pi_1} J_{\mathcal{M}}(\pi)$, we have

$$\mathbb{E}_{\mathcal{M} \sim \mathcal{T}} \max_{\pi \in \Pi_1} J_{\mathcal{M}}(\pi) - \max_{\pi \in \Pi_1} \mathbb{E}_{\mathcal{M} \sim \mathcal{T}} J_{\mathcal{M}}(\pi) \geq \frac{1}{1-\gamma} \mathbb{E}_{s \sim d_{\mathcal{M}, \pi^*}} [D_{\text{TDR}}(\mathcal{T}, s)], \tag{20}$$

Thus we have proven this result. \square

B.3. The Proof of the Inequality (8)

We have

$$\begin{aligned}
 \ln p(o_{1:T}, r_{1:T}, \mathcal{M} | a_{1:T}) &= \ln \mathbb{E}_{p(s_{1:T} | a_{1:T})} [p(o_{1:T}, r_{1:T}, \mathcal{M} | s_{1:T})] \\
 &= \ln \mathbb{E}_{p(s_{1:T} | a_{1:T})} [p(o_{1:T}, r_{1:T} | \mathcal{M}, s_{1:T}) p(\mathcal{M} | o_{1:T}, r_{1:T}, s_{1:T})] \\
 &= \ln \mathbb{E}_{p(s_{1:T} | a_{1:T})} \left[\prod_{t=1}^T p(o_t, r_t | \mathcal{M}, s_t) \right] p(\mathcal{M} | o_{1:T}, r_{1:T}, s_{1:T}) \\
 &= \ln \mathbb{E}_{q(s_{1:T} | o_{1:T}, a_{1:T}, r_{1:T})} \left[\prod_{t=1}^T p(o_t, r_t | \mathcal{M}, s_t) \frac{p(s_t | s_{t-1}, a_{t-1})}{q(s_t | o_{\leq t}, r_{< t}, a_{< t})} \right] p(\mathcal{M} | o_{1:T}, r_{1:T}, s_{1:T}) \\
 &\geq \mathbb{E}_{q(s_{1:T} | o_{1:T}, a_{1:T}, r_{1:T})} \sum_{t=1}^T [\ln p(o_t, r_t | \mathcal{M}, s_t) + \ln p(s_t | s_{t-1}, a_{t-1}) - \ln q(s_t | o_{\leq t}, r_{< t}, a_{< t})] \\
 &\quad + \mathbb{E}_{q(s_{1:T} | o_{1:T}, a_{1:T}, r_{1:T})} \ln p(\mathcal{M} | o_{1:T}, r_{1:T}, s_{1:T}) \\
 &= \sum_{t=1}^T \left[\mathbb{E}_{q(s_{1:T} | o_{1:T}, a_{1:T}, r_{1:T})} \ln p(o_t, r_t | \mathcal{M}, s_t) - \mathbb{E}_{q(s_{1:T} | o_{1:T}, a_{1:T}, r_{1:T})} \ln \frac{q(s_t | o_{\leq t}, r_{< t}, a_{< t})}{p(s_t | s_{t-1}, a_{t-1})} \right] \\
 &\quad + \mathbb{E}_{q(s_{1:T} | o_{1:T}, a_{1:T}, r_{1:T})} \ln p(\mathcal{M} | o_{1:T}, r_{1:T}, s_{1:T}) \\
 &= \sum_{t=1}^T \mathbb{E}_{q(s_t | o_{\leq t}, a_{< t}, r_{< t})} \ln p(o_t, r_t | \mathcal{M}, s_t) \\
 &\quad - \sum_{t=1}^T \mathbb{E}_{q(s_t | o_{\leq t}, r_{< t}, a_{< t})} \mathbb{E}_{q(s_{t-1} | o_{\leq (t-1)}, r_{< (t-1)}, a_{< (t-1)})} \ln \frac{q(s_t | o_{\leq t}, r_{< t}, a_{< t})}{p(s_t | s_{t-1}, a_{t-1})} \\
 &\quad + \mathbb{E}_{q(s_{1:T} | o_{1:T}, a_{1:T}, r_{1:T})} \ln p(\mathcal{M} | o_{1:T}, r_{1:T}, s_{1:T}) \\
 &= \sum_{t=1}^T \mathbb{E}_{q(s_t | o_{\leq t}, a_{< t}, r_{< t})} \ln p(o_t, r_t | \mathcal{M}, s_t) \\
 &\quad - \sum_{t=1}^T \mathbb{E}_{q(s_{t-1} | o_{\leq (t-1)}, r_{< (t-1)}, a_{< (t-1)})} \text{KL}(q(s_t | o_{\leq t}, r_{< t}, a_{< t}) || p(s_t | s_{t-1}, a_{t-1})) \\
 &\quad + \mathbb{E}_{q(s_{1:T} | o_{1:T}, a_{1:T}, r_{1:T})} \ln p(\mathcal{M} | o_{1:T}, r_{1:T}, s_{1:T}).
 \end{aligned} \tag{21}$$

Moreover, we have

$$p(\mathcal{M} | o_{1:T}, r_{1:T}, s_{1:T}) = \frac{p(\mathcal{M}, o_{1:T}, r_{1:T}, s_{1:T})}{p(o_{1:T}, r_{1:T}, s_{1:T})} = p(\mathcal{M} | s_{1:T}) \frac{p(o_{1:T}, r_{1:T} | \mathcal{M}, s_{1:T})}{p(o_{1:T}, r_{1:T} | s_{1:T})}. \tag{22}$$

Thus we have proven the inequality (8).

C. Experimental Details

In this part, we first *roughly* discuss the reward function of tasks in our experiments to better understand their TDR. These reward functions always defined by tolerance function in DeepMind control suite (Tassa et al., 2018), which is a smooth function with parameters $\text{tolerance}(x, \text{bounds} = (\text{lower}, \text{upper}))$ and hope the value of x is within (lower, upper). More details about tolerance function can be found in Tassa et al. (2018).

- **Walker-stand&walk.** This task combination includes two tasks: Walker-stand and Walker-walk, which both require a two-leg robot to maintain its height above a certain threshold, and Walker-walk also hopes it move faster than a certain speed, i.e., their reward functions can be roughly described as

$$\begin{aligned}\mathcal{R}_{\text{stand}} &= \text{tolerance}(\text{height}, (1.2, \infty)), \\ \mathcal{R}_{\text{walk}} &= \text{tolerance}(\text{height}, (1.2, \infty)) * \text{tolerance}(\text{speed}, (1, \infty)).\end{aligned}\quad (23)$$

Therefore, for all states, the optimal action of Walker-walk is also optimal in Walker-stand and TDR here is 0.

- **Cartpole-balance&sparse.** This task combination includes two tasks: Cartpole-balance and Cartpole-balance_sparse, which both hope to balance an unactuated pole with dense and sparse reward respectively. The optimal actions of these tasks are both hope to balance the agent and thus TDR here is 0.
- **Acrobot-swingup&sparse.** This task combination includes two tasks: Acrobot-swingup and Acrobot-swingup_sparse, which both hope to swing up a double pendulum with dense and sparse rewards respectively. Also, the optimal actions of these tasks are both hope to swingup the agent and thus TDR here is 0.
- **Quadruped-walk&run.** This task combination includes two tasks: Quadruped-walk and Quadruped-run, which both require a quadruped agent to move faster than a target speed. The target speed of the running task is larger than the walking task, i.e., their reward functions can be roughly described as

$$\begin{aligned}\mathcal{R}_{\text{walk}} &= \text{tolerance}(\text{speed}, (0.5, \infty)), \\ \mathcal{R}_{\text{run}} &= \text{tolerance}(\text{speed}, (5.0, \infty)).\end{aligned}\quad (24)$$

Therefore, TDR here is still 0 since optimal actions of Quadruped-run are also optimal in Quadruped-walk.

- **Reacher-easy&hard.** This task combination includes two tasks: Reacher-easy and Reacher-hard, which both hope to control a two-link planar reacher to prostrate the target sphere. The sizes of target spheres in two tasks are different, i.e., their reward functions can be roughly described as

$$\begin{aligned}\mathcal{R}_{\text{easy}} &= \text{tolerance}(\text{distance}, (0.0, 0.05)), \\ \mathcal{R}_{\text{hard}} &= \text{tolerance}(\text{distance}, (0.0, 0.015)).\end{aligned}\quad (25)$$

Thus TDR here is not 0 but still small.

- **Hopper-stand&hop.** This task combination includes two tasks: Hopper-stand and Hopper-hop, which both hope the height of a one-legged hopper is larger than the target height. While Hopper-stand hopes the control force is 0, Hopper-hop hopes to control the robot to hop forward and its speed is larger than the target speed. Their reward functions can be roughly described as

$$\begin{aligned}\mathcal{R}_{\text{stand}} &= \text{tolerance}(\text{height}, (0.6, 2)) * \text{tolerance}(\text{speed}, (2.0, \infty)), \\ \mathcal{R}_{\text{hop}} &= \text{tolerance}(\text{height}, (0.6, 2)) * \text{tolerance}(\text{control}, (0.0, 0.0)).\end{aligned}\quad (26)$$

Since one agent can not hop when controlling the force as 0, TDR here is not 0 but not huge.

- **Walker-stand&prostrate.** This task combination includes two tasks: Walker-stand and Walker-prostrate. Walker-stand hopes the height of a two-leg robot to be larger than a target height. And we design the task Walker-prostrate, which hopes its height to be lower than a target height. Their reward functions can be roughly described as

$$\begin{aligned}\mathcal{R}_{\text{stand}} &= \text{tolerance}(\text{height}, (1.2, \infty)), \\ \mathcal{R}_{\text{prostrate}} &= \text{tolerance}(\text{height}, (0.0, 0.2)).\end{aligned}\quad (27)$$

Thus TDR here is huge since optimal Q functions of these two tasks are almost the opposite.

- **Walker-walk&prostrate.** This task combination includes two tasks: Walker-walk and Walker-prostrate. Walker-walk hopes the height of the improved planar walker to be larger than a target height, while Walker-prostrate hopes it to be lower than a target height. Moreover, Walker-walk hopes the speed of the robot is larger than a target speed, i.e., their reward functions can be roughly described as

$$\begin{aligned}\mathcal{R}_{\text{walk}} &= \text{tolerance}(\text{height}, (1.2, \infty)) * \text{tolerance}(\text{speed}, (1.0, \infty)), \\ \mathcal{R}_{\text{prostrate}} &= \text{tolerance}(\text{height}, (0.0, 0.2)).\end{aligned}\tag{28}$$

Thus TDR here is also huge since the optimal Q functions of these two tasks are almost the opposite.

Now we introduce the three task distributions in our experiments, which are designed based on existing tasks in DeepMind control suite for testing the generalization of trained agents.

- **Cheetah_speed(α, β).** This task distribution is designed in this paper with parameter $0 \leq \beta \leq \alpha$, based on the task Cheetah_run in DeepMind control suite, and hopes the Cheetah robot can run with the target speed.

$$\mathcal{R}_{\text{Cheetah_speed}}(\alpha, \beta) = \text{tolerance}(\text{speed}, (\alpha - \beta, \alpha + \beta)).\tag{29}$$

- **Pendulum_angle(α, β).** This task distribution is designed in this paper with parameter $-1 \leq \alpha \leq \beta \leq 1$, based on the task Pendulumh_swingup in DeepMind control suite, and hopes the Pendulum robot can swingup in the target angle.

$$\mathcal{R}_{\text{Pendulum_angle}}(\alpha, \beta) = \text{tolerance}(\text{angle}, (\arccos \alpha, \arccos \beta)).\tag{30}$$

- **Quadruped_speed(α, β).** This task distribution is designed in this paper with parameter $0 \leq \beta \leq \alpha$, based on the task Quadruped_run in DeepMind control suite, and hopes the Quadruped robot can run with the target speed.

$$\mathcal{R}_{\text{Quadruped_speed}}(\alpha, \beta) = \text{tolerance}(\text{speed}, (\alpha - \beta, \alpha + \beta)).\tag{31}$$

Moreover, we introduce some details about our experiments. Our codes are based on Python and the deep learning library PyTorch. All algorithms are trained on one NVIDIA GeForce RTX 2080 Ti. As for the hyper-parameters, we follow previous works (Ha & Schmidhuber, 2018; Hafner et al., 2019b;a) and select 2 as the action repeat for all experiments following (Hafner et al., 2019a).

Ethics Issues and Broader Impacts

Designing agents which can generalize to unseen tasks is a major concern in reinforcement learning. This work focuses on task generalization in reinforcement learning and proposes a novel algorithm Reward Informed Dreamer. One of the potential negative impacts is that algorithms using deep neural networks, which lack interoperability and theoretical guarantee. If we hope to apply them in real-world applications, they may face security and robustness issues, and a possible way is to develop more explainable methods. There are no serious ethical issues as this is basic research. We hope our work can inspire more research on designing agents with stronger generalization abilities.